13 Electronic Collisions in Correlated Systems: From the Atomic to the Thermodynamic Limit

J. Berakdar

13.1 Introduction

This chapter gives a brief overview on recent advances in the treatment of nonrelativistic electronic collisions in finite and extended systems[1]. A proper description of electronic collisions [1–4] is a prerequisite for the understanding of a variety of material properties. Emphasis is put on analytical concepts that unravel common features and differences between scattering events in finite few-body (atomic) systems and large, extended systems (molecules, metal clusters, and solid surfaces). The properties of few-body Coulomb scattering states are discussed for two-, three-, four- and N- particle systems. For large, finite systems the concept of Green's function is utilized as a powerful tool for the description of electronic excitations as well as for the study of collective and thermodynamic properties. For the description of highly excited electronic states in solids and surfaces, the Green's function method, developed in field theory, is used. When available, the theoretical models are contrasted with experimental findings.

13.2 Two Charged-Particle Scattering

For an introduction, we consider the nonrelativistic scattering of two charged particles with charges z_1 and z_2. The Schrödinger equation for the wave function describing the relative motion of the particles is[2]:

$$\left[\Delta - \frac{2\mu z_1 z_2}{r} + k^2\right] \Psi_{\boldsymbol{k}}(\boldsymbol{r}) = 0\,, \tag{13.1}$$

where $\boldsymbol{r}$ is the two-particle relative coordinate and $\boldsymbol{k}$ is the momentum conjugate to $\boldsymbol{r}$. The energy of the relative motion is $E = k^2/2\mu$ and μ is the reduced mass of the particles. The effect of the Coulomb potential is exposed by making the ansatz $\Psi_{\boldsymbol{k}}(\boldsymbol{r}) = \mathrm{e}^{\mathrm{i}\boldsymbol{k}\cdot\boldsymbol{r}}\bar{\Psi}_{\boldsymbol{k}}(\boldsymbol{r})$. The asymptotic behavior of (13.1) is unravelled by neglecting terms that fall off at large r faster than the Coulomb potential, which leads to

$$\left[\mathrm{i}\boldsymbol{k}\cdot\boldsymbol{\nabla} - \frac{\mu z_1 z_2}{r}\right] \bar{\Psi}_{\boldsymbol{k}}(\boldsymbol{r}) = 0\,. \tag{13.2}$$

[1] This work is dedicated to John S. Briggs on the occasion of his sixtieth birthday.

[2] Atomic units are used unless otherwise stated.

This equation admits a solution of the form $\bar{\Psi} = \exp(\mathrm{i}\phi)$, where $\phi_{\boldsymbol{k}}^{\pm}(\boldsymbol{r}) = \pm\frac{z_1 z_2 \mu}{k} \ln k(r \mp \hat{\boldsymbol{k}}\cdot\boldsymbol{r})$. The factor $z_1 z_2 \mu/k = z_1 z_2/v$ (v is the relative velocity) is called the *Sommerfeld parameter* and is a measure for the strength of the interaction potential. The key point is that the natural coordinate for Coulomb scattering is the so-called *parabolic* coordinate $\xi^{\pm} = r \mp \hat{\boldsymbol{k}}\cdot\boldsymbol{r}$, where the signs + or − corresponds to incoming- or outgoing-wave boundary conditions, respectively.

13.3 Three-Particle Coulomb Continuum States

The three-body Coulomb–scattering problem is still receiving much attention [5–15]. This is because, in contrast to the two-body problem, an exact derivation of the three-body quantum states is not possible. Only under certain (asymptotic) assumptions can analytical solutions be obtained that contain some general features of the two-body scattering, such as the characteristic asymptotic phases. As in the preceding section the center-of-mass motion of a three-body system can be factored out. The internal motion of the three charged particles with masses m_i and charges z_i; $i \in 1,2,3$ can be described by one set of the three Jacobi coordinates $(\boldsymbol{r}_{ij}, \boldsymbol{R}_k)$; $i,j,k \in \{1,2,3\}$; $\epsilon_{ijk} \neq 0$; $j > i$. Here, $\boldsymbol{r}_{ij}$ is the relative internal separation of the pair ij, and $\boldsymbol{R}_k$ is the position of the third particle (k) with respect to the center-of-mass of the pair ij. The scalar product

$$(\boldsymbol{r}_{ij}, \boldsymbol{R}_k)\cdot\begin{pmatrix}\boldsymbol{k}_{ij}\\ \boldsymbol{K}_k\end{pmatrix}$$

is invariant for all three sets of Jacobi coordinates. The kinetic energy operator H_0 is then diagonal and reads

$$H_0 = -\Delta_{\boldsymbol{r}_{ij}}/(2\mu_{ij}) - \Delta_{\boldsymbol{R}_k}/(2\mu_k)\,, \quad \forall(\boldsymbol{r}_{ij}, \boldsymbol{R}_k)\,,$$

where $\mu_k = m_k(m_i + m_j)/(m_1 + m_2 + m_3)$ and $\mu_{ij} = m_i m_j/(m_i + m_j)$; $i,j \in \{1,2,3\}$; $j > i$ are reduced masses. The eigenenergy of H_0 is $E_0 = \boldsymbol{k}_{ij}^2/(2\mu_{ij}) + \boldsymbol{K}_k^2/(2\mu_k)$, $\forall(\boldsymbol{k}_{ij}, \boldsymbol{K}_k)$. Defining $z_{ij} = z_i z_j$ the time-independent Schrödinger equation of the system reads

$$\left[H_0 + \sum_{\substack{i,j\\ j>i}}^{3} \frac{z_{ij}}{r_{ij}} - E\right]\langle \boldsymbol{r}_{kl}, \boldsymbol{R}_m | \Psi_{\boldsymbol{k}_{kl}, \boldsymbol{K}_m}\rangle = 0\,. \tag{13.3}$$

The relative coordinates r_{ij} occurring in the Coulomb potentials have to be expressed in terms of the appropriately chosen Jacobi-coordinate set $(\boldsymbol{r}_{kl}, \boldsymbol{R}_m)$.

13.3.1 Coulomb Three-Body Scattering in Parabolic Coordinates

Asymptotic scattering solutions of (13.3) for large interparticle distances $\boldsymbol{r}_{ij}$ have been considered in [5,6,8,9,16]. The derivation of general scattering solutions of the Schrödinger equation is a delicate task. One approach is to consider the three-body system as the subsum of three noninteracting two-body subsystems [11]. Since we know the appropriate coordinates for each of these two-body subsystems (the parabolic coordinates), we formulate the three-body problem in a similar coordinate frame with

$$\{\xi_k^{\mp} = r_{ij} \pm \hat{\boldsymbol{k}}_{ij}\cdot\boldsymbol{r}_{ij}\}\,, \quad \epsilon_{ijk} \neq 0\,; \quad j > i\,, \tag{13.4}$$

where $\hat{\boldsymbol{k}}_{ij}$ denote the directions of the momenta $\boldsymbol{k}_{ij}$. Since we are dealing with a six-dimensional problem, three other independent coordinates are needed in addition to (13.4). To make a reasonable choice for these remaining coordinates we remark that, usually, the momenta $\boldsymbol{k}_{ij}$ are determined experimentally, i.e. they can be considered as the laboratory-fixed coordinates. In fact it can be shown that the coordinates (13.4) are related to the Euler angles. Thus, it is advantageous to choose body-fixed coordinates. Those are conveniently chosen as

$$\{\xi_k = r_{ij}\}\,, \quad \epsilon_{ijk} \neq 0\,; \quad j > i\,. \tag{13.5}$$

Upon a mathematical analysis it can be shown that the coordinates (13.4), (13.5) are linearly independent [11] except for some singular points where the Jacobi determinant vanishes. The main task is now to rewrite the three-body Hamiltonian in the coordinates (13.4) and (13.5). To this end, it is useful to factor out the trivial plane-wave part by making the ansatz

$$\Psi_{\boldsymbol{k}_{ij}, \boldsymbol{K}_k}(\boldsymbol{r}_{ij}, \boldsymbol{R}_k) = N\exp(\mathrm{i}\boldsymbol{r}_{ij}\cdot\boldsymbol{k}_{ij} + \mathrm{i}\boldsymbol{R}_k\cdot\boldsymbol{K}_k)\overline{\Psi}_{\boldsymbol{k}_{ij}, \boldsymbol{K}_k}(\boldsymbol{r}_{ij}, \boldsymbol{R}_k)\,. \tag{13.6}$$

Inserting the ansatz (13.6) into the Schrödinger equation (13.3) leads to

$$\left[\frac{1}{\mu_{ij}}\Delta_{\boldsymbol{r}_{ij}} + \frac{1}{\mu_k}\Delta_{\boldsymbol{R}_k} + 2\mathrm{i}\left(\frac{1}{\mu_{ij}}\boldsymbol{k}_{ij}\cdot\boldsymbol{\nabla}_{\boldsymbol{r}_{ij}} + \frac{1}{\mu_k}\boldsymbol{K}_k\cdot\boldsymbol{\nabla}_{\boldsymbol{R}_k}\right) - 2\sum_{\substack{m,n\\ n>m}}^{3}\frac{Z_{ij}}{r_{mn}}\right]$$
$$\times\overline{\Psi}(\boldsymbol{r}_{ij}, \boldsymbol{R}_k) = 0\,. \tag{13.7}$$

In terms of the coordinates (13.4) and (13.5), (13.7) casts

$$H\overline{\Psi}_{\boldsymbol{k}_{ij}, \boldsymbol{K}_k}(\xi_1, \ldots, \xi_6)$$
$$= [\,H_{\mathrm{par}} + H_{\mathrm{in}} + H_{\mathrm{mix}}]\,\overline{\Psi}_{\boldsymbol{k}_{ij}, \boldsymbol{K}_k}(\xi_1, \ldots, \xi_6) = 0\,. \tag{13.8}$$

The operator H_{par} is differential in the *parabolic* coordinates $\xi_{1,2,3}$ only, whereas H_{int} acts on the internal degrees of freedom $\xi_{4,5,6}$. The mixing term H_{mix} arises from the off-diagonal elements of the metric tensor and plays the role of a rotational coupling in a hyperspherical treatment. The essential

point is that the differential operators $H_{\rm par}$ and $H_{\rm int}$ are exactly separable in the coordinates $\xi_{1\ldots3}$ and $\xi_{4\ldots6}$, respectively, for they can be written as [11]

$$H_{\rm par} = \sum_{j=1}^{3} H_{\xi_j}\,; \quad [H_{\xi_j}, H_{\xi_i}] = 0\,; \quad \forall i,j \in \{1,2,3\}\,, \quad \text{and} \tag{13.9}$$

$$H_{\rm int} = \sum_{j=4}^{6} H_{\xi_j}\,; \quad [H_{\xi_j}, H_{\xi_i}] = 0\,; \quad \forall i,j \in \{4,5,6\}\,, \quad \text{where} \tag{13.10}$$

$$H_{\xi_j} = \frac{2}{\mu_{lm} r_{lm}} \left[\partial_{\xi_j}\xi_j\partial_{\xi_j} + ik_{lm}\xi_j\partial_{\xi_j} - \mu_{lm} z_{lm}\right]\,; \quad \epsilon_{jlm} \neq 0\,; \tag{13.11}$$

$$H_{\xi_4} = \frac{1}{\mu_{23}}\left[\frac{1}{\xi_4^2}\partial_{\xi_4}\xi_4^2\partial_{\xi_4} + i2k_{23}\frac{\xi_1-\xi_4}{\xi_4}\partial_{\xi_4}\right]\,, \tag{13.12}$$

$$H_{\xi_5} = \frac{1}{\mu_{13}}\left[\frac{1}{\xi_5^2}\partial_{\xi_5}\xi_5^2\partial_{\xi_5} + i2k_{13}\frac{\xi_2-\xi_5}{\xi_5}\partial_{\xi_5}\right]\,, \tag{13.13}$$

$$H_{\xi_6} = \frac{1}{\mu_{12}}\left[\frac{1}{\xi_6^2}\partial_{\xi_6}\xi_6^2\,\partial_{\xi_6} + i2k_{12}\frac{\xi_3-\xi_6}{\xi_6}\partial_{\xi_6}\right]\,. \tag{13.14}$$

The operator $H_{\rm mix} = H - H_{\rm par} - H_{\rm int}$ derives from the expression

$$H_{\rm mix} := \sum_{u\neq v=1}^{6} \left\{(\boldsymbol{\nabla}_{\boldsymbol{r}_{ij}}\xi_u)\cdot(\boldsymbol{\nabla}_{\boldsymbol{r}_{ij}}\xi_v) + (\boldsymbol{\nabla}_{\boldsymbol{R}_k}\xi_u)\cdot(\boldsymbol{\nabla}_{\boldsymbol{R}_k}\xi_v)\right\}\partial_{\xi_u}\partial_{\xi_v}\,. \tag{13.15}$$

Noting that $H_{\xi_j}, j = 1,2,3$ is simply the Schrödinger operator for the two-body scattering rewritten in parabolic coordinates (after factoring out the plane-wave part), one arrives immediately, as a consequence of (13.9), at an expression for the three-body wave function as a product of three two-body continuum waves (the so-called 3C-model or the Ψ_{3C} wave function) with the correct boundary conditions at large interparticle separations. This result is valid if the contributions of $H_{\rm int}$ and $H_{\rm mix}$ are negligible as compared to $H_{\rm par}$, which is, in fact, the case for large interparticle separations [11] *or* at high particles' energies. The above procedure can be performed within the Jacobi coordinate system, however, the operators $H_{\rm par}$, $H_{\rm int}$, and $H_{\rm mix}$ have a much more complex representation in the Jacobi coordinates (see [11]).

13.3.2 Remarks on the Structure of the Three-Body Hamiltonian

The structure of (13.9–13.15) and the mathematical properties of the operators $H_{\rm par}$, $H_{\rm int}$, and $H_{\rm mix}$ deserve several remarks.

1. The total potential is contained in the operator $H_{\rm par}$, as can be seen from (13.11). Thus, the eigenstates of $H_{\rm par}$ treat the total potential in an exact manner. This means, on the other hand, that the operators $H_{\rm int}$ and $H_{\rm mix}$ are parts of the kinetic energy operator. This situation is to be contrasted with other treatments of the three-body problem in regions of the space where the potential is smooth, e.g., near a saddle point. In this case one usually expands the potential around the fix point and accounts for the kinetic energy in an exact manner.
2. In (13.11) the total potential appears as a sum of three two-body potentials. It should be stressed that this splitting is arbitrary, since the dynamics is controlled by the total potential. Thus, any other splitting that leaves the total potential invariant is equally justified. We will use this factbelow for the construction of three-body states. For large interparticle separation the operators $H_{\rm int}$ and $H_{\rm mix}$ are negligible as compared to $H_{\rm par}$ and the splitting of the total potential as done in (13.11) becomes unique. For large $k_{ij}r_{ij}$, $\forall ij$, i.e., at high interparticle relative energies the three-body scattering dynamics is controlled by sequential two-body collisions. This is of particular importance for the interpretations of the outcome of experiments that test the three-body continuum problem (see the discussion of the theoretical and experimental results given below).
3. The momentum vectors $\boldsymbol{k}_{ij}$ enter the Schrödinger equation via the asymptotic boundary conditions. Thus, their physical meaning, as two-body relative momenta, is restricted to the asymptotic region of large interparticle distances. The consequence of this conclusion is that, in general, any combination or functional form of the momenta $\boldsymbol{k}_{ij}$ is legitimate, as long as the total energy is conserved and the boundary conditions are fulfilled (the energies and the wave vectors are linked via a parabolic dispersion relation). This fact has been employed in [9] to construct three-body wave functions with position-dependent momenta $\boldsymbol{k}_{ij}$ and in [17] to account for offshell transitions.
4. The separability of the operators (13.12)–(13.14) may be used to deduce representations of three-body states [18] that diagonalize simultaneously $H_{\rm par}$ and $H_{\rm int}$. It should be noted, however, that generally the operator $H_{\rm mix}$, which has to be neglected in this case, falls off with distance as fast as $H_{\rm int}$.
5. As is well known, each separability of a system implies a related conserved quantity. In the present case we can only speak of an approximate separability and hence of approximate conserved quantum numbers. If we discard $H_{\rm int}$ and $H_{\rm mix}$ in favor of $H_{\rm par}$, which is justified for large $k_{ij}\xi_k$, $\epsilon_{ijk} \neq 0, k \in [1,3]$ (i.e., for large ξ_k or for high two-particle momenta k_{ij}), the three-body good quantum numbers are related to those in a two-body system in parabolic coordinates. The latter are the two-body energy, the eigenvalue of the component of the Lenz–Runge operator along a quantization axis z, and the eigenvalue of the component of the angular momentum operator along z. In our case the quantization axis z is given by the linear momentum direction $\hat{\boldsymbol{k}}_{ij}$. In [11] the three-body problem has been formulated in hyperspherical-parabolic coordinates. In this case, the operator $H_{\rm int}$ takes on the form of the grand angular momentum opera-

tor. This observation is useful to expose the relevant angular momentum quantum numbers in case $H_{\rm mix}$ can be neglected.

6. In [8] the three-body system has been expressed in the coordinates $\eta_j = \xi_j^+$, $j = 1,2,3$ and $\bar{\eta}_j = \xi_j^-$, $j = 1,2,3$. From a physical point of view this choice is not quite suitable, for scattering states are sufficiently quantified by outgoing- or incoming-wave boundary conditions (in contrast to standing waves, such as bound states whose representation requires a combination of incoming and outgoing waves). Therefore, to account for the boundary conditions in scattering problems, either the coordinates η_j or $\bar{\eta}_j$ are needed. The appropriate choice of the remaining three coordinates should be made on the basis of the form of the forces governing the three-body system. In the present case where external fields are absent we have chosen $\xi_k = r_{ij}$, $k = 4,5,6$ as the natural coordinates adopted to the potential energy operator.
7. The approximate separability of the three-body Hamiltonian in the high energy regime (see (13.12)–(13.14)) results in the commutation relation of the two-body Hamiltonians $[H_{\xi_i}, H_{\xi_j}]$, $i,j \in \{1,2,3\}$. This fact can be expressed in terms of Green operators, which offers a connection to well-established methods of many-body theories [19,20] (see below for a brief summary of the Green's function method): let $G^{(3)}(z) = (z - H)^{-1}$ be the Green operator of the system. In a three-body system we consider, in a first step, two particles, say particle 1 and particle 2 to move independently *and* on the two-body energy-shell in the field of particle 3. In this case we find $G^{(3)} = g_1\, g_2$, where $g_{1/2}$ are the two-body Green operators describing the independent motion of the respective particles. At high interparticle relative energies we can write $H = H_{\rm par} = \sum_{j=1}^{3} H_{\xi_j}$ (see (13.8)). In Green's function language this means

$$G^{(3)} \approx G^{(3)}_{\rm 3C} = g_1\,(I + g_{12}\, v_{12})\; g_2\,, \tag{13.16}$$

where v_{12} is the interaction potential between the particles 1 and 2 and $g_{12} = G_0 + G_0 v_{12} g_{12} = G_0 + G_0 v_{12} G_0 + G_0 v_{12} G_0 v_{12} G_0 + \cdots$. Here G_0 is the Green's operator in absence of interactions. Upon insertion of g_{12} in (13.16) and noting that $G_0(z) = (z - H_0)^{-1}$ we obtain

$$G^{(3)} \approx g_1 g_2 + g_1\,\kappa_{12}\, g_2 + g_1\,\kappa_{12}\,\kappa_{12}\, g_2 + g_1\,\kappa_{12}\,\kappa_{12}\,\kappa_{12}\, g_2 \cdots\,, \tag{13.17}$$

where κ_{12} is a dimensionless coupling parameter that measures the strength of the interaction potential (v_{12}) as compared to the kinetic energy (H_0). From (13.17) the following picture emerges: particle 1 and 2 can be considered as quasiparticles that interact successively an infinite number of times via κ_{12}. This is the exact counterpart of what is known as the *ladder approximation* in many-body theory [19,20]. This means that the approximation $G^{(3)} \approx G^{(3)}_{\rm 3C}$ amounts to an exact sum of all the ladder diagrams. On the other hand, it is documented [19,20] that the ladder approximation results upon disregarding a number of (crossed) diagrams

that are as well not accounted for by $G^{(3)}_{\rm 3C}$ for the three-body case. A way to incorporate these "higher-order" many-body effects is to consider them as a renormalization of the single-particle properties (mass, charge, etc.) and of the two-body interactions (v_{12}). The renormalized single-particle Green's functions and the mutual interaction are labeled, respectively, by $\tilde{g}_{1/2}$ and $\tilde{v}_{12}$. This procedure is outlined in the next section.

13.3.3 Dynamical Screening

In the realm of many-body theory it is well established that under certain conditions (small perturbations, low excitations) interaction effects can be accounted for by renormalizing the single-particle properties so that the one-particle picture remains viable. In the context of the three-body problem these ideas can be utilized and generalized as follows: correlations effects whose description goes beyond the ladder approximation should be incorporated as a redefinition of the two-particle properties so that we can still operate within the ladder approximation. In terms of wave functions this means we seek three-body wave functions that are eigenfunctions not only of $H_{\rm par}$, but also of parts of $H_{\rm int}$ and $H_{\rm mix}$. In addition, the structure of the total Hamiltonian, in the sense of (13.9) and (13.11), should be maintained.

As it turned out this can be achieved by introducing renormalized two-particle coupling strengths, namely, instead of z_{ij} for the bare two-body interaction, we define a variable $\bar{z}_{ij}$ and determine its functional dependence such that the structure of (13.9) and (13.11) is preserved. Using these $\bar{z}_{ij}$ one can then write down the three-body Green's operator in terms of the *dressed* one-particle Green's operators $\tilde{g}_{1/2}$, e.g., $\tilde{g}_1 = g_{01} + g_{01}\,(\tilde{z}_{13}/r_{13})\, g_1$, where g_{01} is the free Green's operator of particle 1 and r_{13} is the relative position of particle 1 with respect to particle 3.

The actual derivation of $\bar{z}_{ij}$ is quite involved and is based on the following observations. (i) In a three-body system the form of the two-body potentials z_{ij}/r_{ij} are generally irrelevant, as long as the total potential is conserved. (ii) To keep the mathematical structure of the operators (13.9) and (13.11) unchanged and to introduce a splitting of the total potential, while maintaining the total potential's rotational invariance, one assumes the strength of the individual two-body interactions, characterized by z_{ij}, to be dependent on $\xi_{4,5,6}$. This means we introduce position-dependent product charges as $\bar{z}_{ij} = \bar{z}_{ij}(\xi_4, \xi_5, \xi_6)$, with $\sum_{j>i=1}^{3} \frac{\bar{z}_{ij}}{r_{ij}} = \sum_{j>i=1}^{3} \frac{z_{ij}}{r_{ij}}$. To obtain the "re-normalized" *many-body* potentials $\bar{V}_{ij} := \bar{z}_{ij}/r_{ij}$ we write $\bar{V}_{ij}$ as a linear combination of the isolated *two-body* interactions $V_{ij} := z_{ij}/r_{ij}$, i.e.,

$$\begin{pmatrix} \bar{V}_{23} \\ \bar{V}_{13} \\ \bar{V}_{12} \end{pmatrix} = \mathcal{A} \begin{pmatrix} V_{23} \\ V_{13} \\ V_{12} \end{pmatrix}\,, \tag{13.18}$$

where $\mathcal{A}(\xi_4, \xi_5, \xi_6)$ is a 3×3 matrix. The matrix elements are then determined according to (1) the properties of the total potential surface, (2) to

reproduce the correct asymptotic of the three-body states and (3) in a way that minimizes $H_{\rm int}$ and $H_{\rm mix}$. It should be stressed that the procedure until this stage is exact. It is merely a splitting of the total potential that leaves this potential and hence the three-body Schrödinger equation unchanged.

For an electron pair moving in the field of a positive ion the determination of $\bar{z}_{ij}$ has been accomplished in [10,11,21]. The resulting wave function has been termed the dynamically screened three-body continuum wave function (DS3C) $\Psi_{\rm DS3C}$.

13.4 Theory of Excited N-Particle Finite Systems

Unfortunately, the curvilinear coordinate system (13.4), (13.5) used for the three-body problem does not have a straightforward generalization to the N–body case. The speciality of the three-body problem is that the number of interaction lines is equal to the number of particles. Therefore, the N-body Coulomb scattering problem has to be approached differently. For large N our system resembles that of the interacting electron gas (EG). In contrast to the present case, however, conventional treatments of EG [1,3,19] are focused on ground-state properties and (low-energy) excitations in the linear response regime.

13.5 Continuum States of N-Charged Particles

The motion of $N-1$ charged particles (with charges z_j, $j \in [1, N-1]$) in the field of a massive residual ion with charge z, at energies above the complete fragmentation threshold, is described by the Schrödinger equation

$$\left[H_0 + \sum_{j=1}^{N} \frac{z z_j}{r_j} + \sum_{\substack{i,j \\ j>i=1}}^{N} \frac{z_i z_j}{r_{ij}} - E\right] \Psi(\boldsymbol{r}_1, \cdots, \boldsymbol{r}_N) = 0\,, \tag{13.19}$$

where $\boldsymbol{r}_j$ is the position of particle j with respect to the residual charge z and $\boldsymbol{r}_{ij} = \boldsymbol{r}_i - \boldsymbol{r}_j$ denotes the relative coordinate between particles i and j. The kinetic energy operator H_0 has the form (in the limit $m/M \to 0$, where M is the mass of the charge z and m is the mass of the continuum particles, which are assumed to have equal masses) $H_0 = -\sum_{\ell=1}^{N} \Delta_\ell/2m$, where Δ_ℓ is the Laplacian with respect to the coordinate $\boldsymbol{r}_\ell$. We note here that for a system of general masses the problem is complicated by an additional mass-polarization term that arises in (13.19). Upon introduction of N-body Jacobi coordinates, H_0 becomes diagonal, however, the potential terms acquire a much more complex form. The continuum states are characterized by the $N-1$ asymptotic momentum vectors $\boldsymbol{k}_j$. The Sommerfeld parameters α_j, α_{ij} are given by $\alpha_{ij} = \frac{z_i z_j}{v_{ij}}$, $\alpha_j = \frac{z z_j}{v_j}$.

Here, $\boldsymbol{v}_j$ is the velocity of the particle j and $\boldsymbol{v}_{ij} := \mathbf{v_i} - \mathbf{v_j}$. The total energy of the system E is given by the asymptotic value of the kinetic energy, i.e., $E = \sum_{l=1}^{N} E_l$, where $E_l = \frac{k_l^2}{2m}$. Scattering eigenstates $\Psi(\boldsymbol{r}_1, \cdots, \boldsymbol{r}_N)$ of (13.19) have been derived using the ansatz [15]

$$\Psi(\boldsymbol{r}_1, \cdots, \boldsymbol{r}_N) = \mathcal{N} \Phi_I(\boldsymbol{r}_1, \cdots, \boldsymbol{r}_N) \Phi_{II}(\boldsymbol{r}_1, \cdots, \boldsymbol{r}_N) \chi(\boldsymbol{r}_1, \cdots, \boldsymbol{r}_N)\,, \tag{13.20}$$

where Φ_I, Φ_{II} are appropriately chosen functions, $\mathcal{N}$ is a normalization constant and $\chi(\boldsymbol{r}_1, \cdots, \boldsymbol{r}_N)$ is a function of an arbitrary form. The function Φ_I is chosen to describe the motion of N-independent Coulomb particles moving in the field of the charge z at the total energy E, i.e., Φ_I is determined by the differential equation

$$\left(H_0 + \sum_{j=1}^{N} \frac{z z_j}{r_j} - E\right) \Phi_I(\boldsymbol{r}_1, \cdots, \boldsymbol{r}_N) = 0\,. \tag{13.21}$$

The regular solution Φ_I is $\Phi_I(\boldsymbol{r}_1, \cdots, \boldsymbol{r}_N) = \prod_{j=1}^{N} \bar{\xi}_j(\boldsymbol{r}_j) \varphi_j(\boldsymbol{r}_j)$, where $\bar{\xi}_j(\boldsymbol{r}_j)$ is a plane wave dependent on the coordinate $\boldsymbol{r}_j$ and characterized by the wave vector $\boldsymbol{k}_j$. Furthermore, $\varphi_j(\boldsymbol{r}_j)$ is a confluent-hypergeometric function in the notation of [22] $\varphi_j(\boldsymbol{r}_j) =_1 F_1[\alpha_j, 1, -\mathrm{i}(k_j r_j + \boldsymbol{k}_j \cdot \boldsymbol{r}_j)]$. The function Φ_I describes the motion of the continuum particles in the extreme case of very strong coupling to the residual ion, i.e., $|z z_j| \gg |z_j z_i|$; $\forall i, j \in [1, N-1]$. In order to incorporate the other extreme case of strong correlations among the continuum particles ($|z_j z_i| \gg |z z_j|$; $\forall i, j \in [1, N-1]$) we choose Φ_{II} to possess the form

$$\begin{aligned} \Phi_{II}(\boldsymbol{r}_1, \cdots, \boldsymbol{r}_N) &= \overline{\Phi}_{II}(\boldsymbol{r}_1, \cdots, \boldsymbol{r}_N) \prod_{j=1}^{N} \bar{\xi}_j(\boldsymbol{r}_j)\,, \\ \overline{\Phi}_{II}(\boldsymbol{r}_1, \cdots, \boldsymbol{r}_N) &= \prod_{j>i=1}^{N} \varphi_{ij}(\boldsymbol{r}_{ij})\,, \end{aligned} \tag{13.22}$$

where $\varphi_{ij}(\boldsymbol{r}_{ij}) :=_1 F_1[\alpha_{ij}, 1, -\mathrm{i}(k_{ij} r_{ij} + \boldsymbol{k}_{ij} \cdot \boldsymbol{r}_{ij})]$. It is straightforward to show that the expression $\varphi_{ij}(\boldsymbol{r}_{ij}) \prod_{l=1}^{N} \bar{\xi}_l(\boldsymbol{r}_l)$ solves for the Schrödinger equation (13.19) in the case of extreme correlations between particle i and particle j, i.e., $|z z_l| \ll |z_i z_j| \gg |z_m z_n|$, $\forall l, m, n \neq i, j$. In terms of differential equations this means

$$\left(H_0 + \frac{z_i z_j}{r_{ij}} - E\right) \varphi_{ij}(\boldsymbol{r}_{ij}) \prod_{j=1}^{N} \bar{\xi}_j(\boldsymbol{r}_j) = 0\,. \tag{13.23}$$

It should be stressed, however, that the function (13.22) does not solve for (13.19) in the case of weak coupling to the residual ion ($z \to 0$), but otherwise comparable strength of correlations between the continuum particles, because the two-body subsystems formed by the continuum particles are coupled to each other. This is the equivalent situation to the interacting electron gas.

The determination of the properties of the function χ that occurs in the ansatz (13.20) is a lengthly procedure and has been discussed in full detail in [15]. It turned out that, at higher energies or at large interparticle distances, χ has the form of a product of plane waves. In general, however, no closed analytical expression for χ has been found yet.

13.6 Green Function Theory of Finite Correlated Systems

With increasing number of particles the treatment of correlated systems becomes more complex and new phenomena appear whose description requires the knowledge of the collective behavior of the system. Thus, an approach is needed that is different from the wave function treatment. The method of choice for this purpose is the Green–function technique, which we will outline in this section.

A principle task in many-body systems is to deal appropriately with the correlations between the particles, for the independent-particle problem can be solved is a standard way. Therefore, for a canonical ensemble, a non-perturbative method has been developed [23] that allows dilution of the interparticle interaction strength to a level where the problem can be solved by conventional methods (perturbation theory, mean-field approach, etc.). This can be achieved by an incremental procedure in which the N correlated particle system is mapped exactly onto a set of systems in which only $N-M$ particles are interacting ($M \in [1, N-2]$), i.e., in which the strength of the potential energy part is damped.

The total potential is assumed to be of the class $U^{(N)} = \sum_{j>i=1}^{N} v_{ij}$ without any further specification of the individual potentials v_{ij}. The key point is that the potential $U^{(N)}$ satisfies the recurrence relations

$$U^{(N)} = \frac{1}{N-2}\sum_{j=1}^{N} u_j^{(N-1)}, u_j^{(N-1)} = \frac{1}{N-3}\sum_{k=1}^{N-1} u_{jk}^{(N-2)}, \quad j \neq k, \tag{13.24}$$

where $u_j^{(N-1)}$ is the total potential of a system of $(N-1)$ interacting particles in which the j particle is missing ($u_j^{(N-1)} = \sum_{m>n=1}^{N} v_{mn}$, $m \neq j \neq n$).

As shown in [23] the decomposition (13.24) can be used to derive similar recurrence relations for the transition $T^{(N)}$ and the Green's operator $G^{(N)}$, namely $T^{(N)} = \sum_{j=1}^{N} T_j^{(N-1)}$, $j \in [1, N]$ and

$$\begin{pmatrix} T_1^{(N-1)} \\ T_2^{(N-1)} \\ \vdots \\ T_{N-1}^{(N-1)} \\ T_N^{(N-1)} \end{pmatrix} = \begin{pmatrix} t_1^{(N-1)} \\ t_2^{(N-1)} \\ \vdots \\ t_{N-1}^{(N-1)} \\ t_N^{(N-1)} \end{pmatrix} + [\boldsymbol{K}^{(N-1)}] \begin{pmatrix} T_1^{(N-1)} \\ T_2^{(N-1)} \\ \vdots \\ T_{N-1}^{(N-1)} \\ T_N^{(N-1)} \end{pmatrix}. \tag{13.25}$$

Here, $t_j^{(N-1)}$ is the transition operator of a system, in which only $N-1$ particles are interacting. The kernel $[\boldsymbol{K}^{(N-1)}]$ is given in terms of $t_j^{(N-1)}$ only [23]. From (13.24) it is clear that $t_j^{(N-1)}$ can also be expressed in terms of the transition operators of the system where only $(N-2)$ particles are interacting leading to a recursive scheme. From the relation $G^{(N)} = G_0 + G_0 T^{(N)} G_0$ similar conclusions are made for the Green operator $G^{(N)} = G_0 + \sum_{j=1}^{N} G_j^{(N-1)}$. The operators $G_j^{(N-1)}$ are related to the Green operators $g_j^{(N-1)}$ of the systems in which only $(N-1)$ particles are correlated.

13.6.1 Application to Four-Body Systems

For the four-body system, $G^{(4)}$ can be expressed in terms of three-body Green's functions, namely, $G^{(4)} = \sum_{j=1}^{4} g_j^{(3)} - 3G_0$. Here, $g_j^{(3)}$ is the Green operator of the system where only three particles are interacting. In terms of state vectors the above procedure amounts to $|\Psi^{(4)}\rangle = |\psi_{234}^{(3)}\rangle + |\psi_{134}^{(3)}\rangle + |\psi_{124}^{(3)}\rangle + |\psi_{123}^{(3)}\rangle - 3|\phi_{\text{free}}^{(4)}\rangle$, where $|\psi_{ijk}^{(3)}\rangle$ is the state vector of the system in which the three particles i, j, and k are interacting, whereas $|\phi_{\text{free}}^{(4)}\rangle$ is the state vector of the noninteracting four-body system. Here, $|\psi_{ijk}^{(3)}\rangle$ is assumed known.

13.6.2 Thermodynamics and Phase Transitions in Finite Systems

Strictly speaking, finite systems do not exhibit phase transitions [24]. However, one expects to observe the onset of a critical behavior when the system approaches the thermodynamic limit. The traditional theory concerned with these questions is finite-size scaling theory [26]. For interacting systems the methods outlined above together with the ideas developed in [24,25], can be utilized for the study of critical phenomena in finite correlated systems: The canonical partition function is expressed in terms of the many-body Green function as $Z(\beta) = \int \mathrm{d}E\ \Omega(E)\ \mathrm{e}^{-\beta E}$. Here, $\Omega(E)$ is the density of states that is related to the imaginary part of the trace of $G^{(N)}$ via $\Omega(E) = -\frac{1}{\pi}\boldsymbol{Tr}\Im G^{(N)}(E)$. The recurrence relation outlined above for the N-body Green function can be utilized to calculate $\Omega(E)$, leading to a recursion relation for the partition function

$$Z^{(N)} = \sum_{j=1}^{N} Z_j^{(N-1)} - (N-1)Z_0. \tag{13.26}$$

Here, Z_0 is the partition function of the independent particle system (taken as a reference), while $Z_j^{(N-1)}$ is the canonical partition function of a system in which the interaction strength is diluted by cutting all interaction lines that connect to particle j. Equation (13.26) allows the thermodynamic properties

of finite systems to be studied on a microscopic level as well as investigation of the inter-relation between the thermodynamics and the strength of correlations. Critical phenomena can be studied using the idea put forward by Yang and Lee [24,25]. For example, if one is interested in the onset of condensation in a quantum Bose gas, the ground-state occupation number $\eta_0(N,\beta)$ has to be considered

$$\eta_0(N,\beta) = -\frac{1}{\beta}\frac{\partial_{\epsilon_0} Z^{(N)}(\beta)}{Z^{(N)}(\beta)} = -\frac{1}{\beta}\frac{\sum_{j=1}^{N}\partial_{\epsilon_0} Z_j^{(N-1)} - (N-1)\partial_{\epsilon_0} Z_0}{Z^{(N)}}\,. \tag{13.27}$$

Here, ϵ_0 is the ground-state energy. By means of this equation one can study systematically the influence of the interaction on the onset of the critical regime or one may chose to find the roots of (13.26) in the complex β plane. Zero points of $Z^{(N)}(\beta)$ that approach systematically the real β axis signify the presence of transition points in the thermodynamic limit.

13.7 Collective Response Versus Short-Range Dynamics

In the thermodynamic limit (large volume V, large N, and finite number density $n = N/V$) the characteristic response of the system will be dominated by the cooperative behavior of all the electrons. For example, the fluctuations of the electronic density are determined by the polarization operator $\Pi(\boldsymbol{q},\omega)$, which depends on the momentum transfer $\boldsymbol{q}$ and the frequency ω. On the other hand, the polarization of the medium modifies the properties of the particle–particle interaction $U(\boldsymbol{q},\omega)$. The modified potential U_{eff} is related to U and $\Pi(\boldsymbol{q},\omega)$ through the integral equation [2,3], i.e., $U_{\text{eff}} = U + U\Pi U_{\text{eff}}$; or $U_{\text{eff}} = U/(1 - U\Pi)$. Thus, the *screening* is quantified by $\kappa(\boldsymbol{q},\omega) = 1/(1 - U\Pi)$, which is called the generalized dielectric function [3]. To determine U_{eff} and κ one needs the polarization function Π that describes the particle–hole excitations. The lowest-order approximation Π_0 is given by the random-phase approximation (RPA) as $\mathrm{i}\Pi_0(\boldsymbol{q},\omega) = \frac{2}{(2\pi)^4}\int \mathrm{d}\boldsymbol{p}\mathrm{d}\xi G_0(\boldsymbol{q}+\boldsymbol{p},\omega+\xi)G_0(\boldsymbol{p},\xi)$. Here G_0 is the free, single-particle Green function. The evaluation of Π_0 can be performed analytically for a homogeneous system [3]. In the long wavelength limit we have $\Pi_0 \approx -2N(\mu)$, where $N(\mu)$ is the density of states at the Fermi level μ. This means that, in the presence of the medium, the electron–electron interaction has the form $U_{\text{TF}} = 4\pi/[q^2 + 8\pi N(\mu)]$. In configuration space one obtains $U_{\text{TF}} = \mathrm{e}^{-r/\lambda}/r$.

Hence, in contrast to atomic systems where collisions with small momentum transfer are predominant ($U \propto 1/q^2$), in a polarizable medium scattering events with small q are cut out due to the finite range of the renormalized scattering potential U_{eff}. The essential difference between the screening effects we are dealing with here and those introduced in the context of the DS3C theory is that in the DS3C screening is incorporated into an explicit many-body theory to account for higher-order diagrams (beyond the ladder approximation) whereas here the screening accounts for certain correlations effects (linear response theory) within a mean-field theory.

Apart from the case of the extended, homogeneous electron gas the evaluations of U_{eff} is generally a challenging task (plane waves are, in general, not the single-particle eigenstates of the system). For an inhomogeneous electronic system, like solids and surfaces, the GW approximation [27] offers a direct extension of the RPA (G stands for the Green's function and $W \equiv U_{\text{eff}}$ for the screened interaction). In [28] this scheme has been discussed and results for the dielectric functions of copper and nickel surfaces have been presented.

13.7.1 Manifestations of Collective Response in Finite Systems

For finite systems the spectrum is generally discrete, which hinders fluctuations around the ground state. However, on increasing the size and number density n collective effects set in. The influence of the fluctuations is demonstrated nicely when considering the ionization channel of large molecules or metal clusters upon electron impact. Within the RPAE (RPA with exchange) the screened interaction U_{eff} between the electron and the target is

$$\begin{aligned}\left\langle \boldsymbol{k}_1\boldsymbol{k}_2 \left| U_{\text{eff}} \right| \phi_\nu \boldsymbol{k}_0 \right\rangle &= \left\langle \boldsymbol{k}_1\boldsymbol{k}_2 \left| U \right| \phi_\nu \boldsymbol{k}_0 \right\rangle \\ &+ \sum_{\substack{\varepsilon_\mathrm{p}\le\mu \\ \varepsilon_\mathrm{h}>\mu}} \left(\frac{\left\langle \varphi_\mathrm{p}\boldsymbol{k}_2 \left| U_{\text{eff}} \right| \phi_\nu\varphi_\mathrm{h} \right\rangle \left\langle \varphi_\mathrm{h}\boldsymbol{k}_1 \left| U \right| \boldsymbol{k}_0\varphi_\mathrm{p} \right\rangle}{\epsilon_0 - (\varepsilon_\mathrm{p} - \varepsilon_\mathrm{h} - \mathrm{i}\delta)} \right. \\ &\left. - \frac{\left\langle \varphi_\mathrm{h}\boldsymbol{k}_2 \left| U_{\text{eff}} \right| \phi_\nu\varphi_\mathrm{p} \right\rangle \left\langle \varphi_\mathrm{p}\boldsymbol{k}_1 \left| U \right| \boldsymbol{k}_0\varphi_\mathrm{h} \right\rangle}{\epsilon_0 + (\varepsilon_\mathrm{p} - \varepsilon_\mathrm{h} - \mathrm{i}\delta)} \right)\,.\end{aligned} \tag{13.28}$$

φ_p and φ_h are, respectively, the intermediate particle's and hole's states with the energies ε_p, ε_h, whereas δ is a small positive real number and μ is the chemical potential. The first term of (13.29) on the RHS amounts to neglecting the electron–hole (de)excitations, as done in [30]. In [29] (13.29) has been evaluated self-consistently for the C_{60} cluster and the ionization cross section has been calculated. The results are shown in Fig. 13.1, which clearly demonstrates the significance of screening in shrinking the effective size of the scattering region and thus leading to a suppression of the ionization cross section.

13.8 The Quantum Field Approach: Basic Concepts

For strongly correlated systems or multiple excitations in extended systems (such as one-electron or one-photon double–electron emission (γ, 2e) or (e,2e))

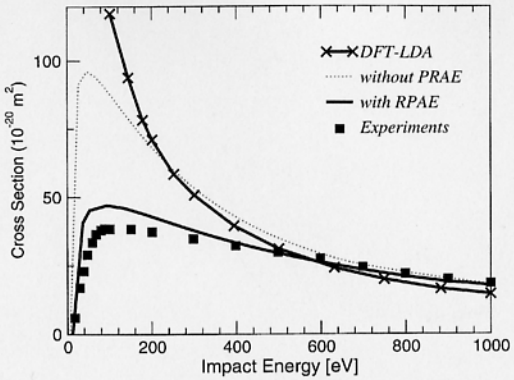

Fig. 13.1. Total electron-impact ionization cross section of C_{60} as a function of the impact energy. The *absolute* experimental data (*full squares*) for the production of stable C_{60}^+ [31,32] are shown. The *solid line with crosses* is the DFT results [33], the *dotted line (solid)* is the result of the present calculation without RPAE (with RPAE)

methods that go beyond RPA are needed. There are a number of theories available, however most of them, like the hole-line expansion or the coupled-cluster methods [3,4,34], are restricted to the treatment of ground-state properties. For the treatment of correlated excited states the Green's function approach is well suited, however, the method as introduced in previous sections, becomes intractable with increasing N, since in this case one works within first quantization, i.e., the states have to be (anti)symmetrized.

Applying methods of field theory, Migdal and Galitskii as well as Martin and Schwinger [35,36] developed a theory that connects, by means of Feynman diagrams, higher-order propagators to the single particle (sp) propagator. The latter is then related to the free unperturbed propagator. The system symmetry enters through (anti)commutation relations of the operators [3,19,20]. This (perturbative) route has found extensive applications in various fields of physics. Here, we focus on the aspects that are of immediate relevance to $(\gamma, 2e)$ and (e,2e) reactions.

13.8.1 The Single–Particle Green's Function for Extended Systems

The sp Green's function $g(\alpha t, \beta t')$ can be considered as an expectation value for the time-ordered product of two operators evaluated using the correlated, exact (normalized) ground state $|\Psi_0\rangle$ of the N electron system, i.e.,

$$\mathrm{i}g(\alpha t, \beta t') = \langle\Psi_0|\mathcal{T}[a_{\mathrm{H}\alpha}(t)a^\dagger_{\mathrm{H}\beta}(t')]|\Psi_0\rangle\,,$$

where $\mathcal{T}$ is the time-ordering operator. $a^\dagger_{\mathrm{H}\beta}(t')$ and $a_{\mathrm{H}\alpha}(t)$ stand, respectively, for the fermionic creation and annihilation operators in the Heisenberg picture represented in an appropriate basis, the members of which are characterized by quantum numbers α and β. For a translationally invariant system, the appropriate basis states are the momentum eigenstates, labeled by $\boldsymbol{k}$. The effect of the chronological operator $\mathcal{T}$ can be described in terms of the step function $\Theta(t-t')$, in which case the Green's function is given by

$$\begin{aligned}\mathrm{i}g(k,t-t') &= \Theta(t-t')\langle\Psi_0|a_{\mathrm{H}k}(t)a^\dagger_{\mathrm{H}k}(t')|\Psi_0\rangle \\ &\quad -\Theta(t'-t)\langle\Psi_0|a^\dagger_{\mathrm{H}k}(t')a_{\mathrm{H}k}(t)|\Psi_0\rangle \\ &= \Theta(t-t')\sum_\gamma \mathrm{e}^{-\mathrm{i}[E^{(N+1)}_\gamma - E^{(N)}_0](t-t')}\left|\langle\Psi^{(N+1)}_\gamma|a^\dagger_k|\Psi_0\rangle\right|^2 \\ &\quad -\Theta(t'-t)\sum_\delta \mathrm{e}^{-\mathrm{i}[E^{(N)}_0 - E^{(N-1)}_\delta](t-t')}\left|\langle\Psi^{(N-1)}_\delta|a_k|\Psi_0\rangle\right|^2 .\end{aligned} \tag{13.29}$$

$\Psi^{(N+1)}_\gamma$ and $\Psi^{(N-1)}_\delta$ stand for a complete set of eigenstates of the $(N+1)$- and the $(N-1)$ particle system, respectively. The energies $E^{(N)}_0$, $E^{(N+1)}_\gamma$, and $E^{(N-1)}_\delta$ refer to the exact energies for the correlated ground state of, respectively, the N, the $(N+1)$, and the $(N-1)$ particle system. The exponential with the energies in (13.30) is due to the Hamiltonians in the exponential functions in the definition of the Heisenberg operators. Noting that the step function has the integral representation

$$\Theta(t) = -\lim_{\eta\to 0}\frac{1}{2\pi\mathrm{i}}\int_{-\infty}^{\infty}\mathrm{d}\omega\frac{\mathrm{e}^{-\mathrm{i}\omega t}}{\omega+\mathrm{i}\eta}\,,$$

the Green's function in energy space can be obtained via Fourier transforming the time difference $t-t'$ to the energy variable ω. This yields the spectral or Lehmann representation of the sp Green's function [37],

$$\begin{aligned}g(k,\omega) = \lim_{\eta\to 0}\Bigg[&\sum_\gamma \frac{\left|\langle\Psi^{(N+1)}_\gamma|a^\dagger_k|\Psi_0\rangle\right|^2}{\omega-[E^{(N+1)}_\gamma - E^{(N)}_0]+\mathrm{i}\eta} \\ &+\sum_\delta \frac{\left|\langle\Psi^{(N-1)}_\delta|a_k|\Psi_0\rangle\right|^2}{\omega-[E^{(N)}_0 - E^{(N-1)}_\delta]-\mathrm{i}\eta}\Bigg]\,.\end{aligned} \tag{13.30}$$

This relation underlines that the sp Green's function is expressible in terms of measurable quantities: the poles of $g(k,\omega)$ correspond to the change in energy (with respect to $E^{(N)}_0$) if one particle is added $(E^{(N+1)}_\gamma - E^{(N)}_0)$ or one particle is removed $(E^{(N)}_0 - E^{(N-1)}_\delta)$ from the reference ground state with N interacting particle. The residua of these poles are given by the *spectroscopic factors*, i.e., the measurable probabilities of adding and removing one particle

with wave vector $\boldsymbol{k}$ to produce the specific state γ (δ) of the residual system. Clearly, the latter probability is of direct relevance to the (e,2e) process. The infinitesimal quantity η shifts the poles below the Fermi energy (the states of the $(N-1)$ system) to slightly above the real axis and those above the Fermi energy [the states of the $(N+1)$ system] to slightly below the real axis.

It is useful to write the single-particle Green's function in terms of the hole and particle spectral functions, which are given for $\omega \leq \epsilon_{\mathrm{F}}$ by

$$S_{\mathrm{h}}(k,\omega) = \frac{1}{\pi}\Im g(k,\omega) = \sum_{\gamma} \left|\langle \Psi_{\gamma}^{(N-1)}|a_k|\Psi_0\rangle\right|^2 \delta(\omega - (E_0^{(N)} - E_{\gamma}^{(N-1)}))\,, \tag{13.31}$$

and for $\bar{\omega} > \epsilon_{\mathrm{F}}$

$$S_{\mathrm{p}}(k,\bar{\omega}) = \frac{1}{\pi}\Im g(k,\bar{\omega}) = \sum_{\gamma} \left|\langle \Psi_{\gamma}^{(N+1)}|a_k^{\dagger}|\Psi_0\rangle\right|^2 \delta(\bar{\omega} - (E_{\gamma}^{(N+1)} - E_0^{(N)}))\,. \tag{13.32}$$

The sp Green's function is then written as

$$g(k,\omega) = \lim_{\eta\to 0}\left(\int_{-\infty}^{\epsilon_{\mathrm{F}}} \mathrm{d}\omega' \frac{S_{\mathrm{h}}(k,\omega')}{\omega - \omega' - \mathrm{i}\eta} + \int_{\epsilon_{\mathrm{F}}}^{\infty} \mathrm{d}\omega' \frac{S_{\mathrm{p}}(k,\omega')}{\omega - \omega' + \mathrm{i}\eta}\right). \tag{13.33}$$

The single-particle Green's function is particularly important since it establishes a direct link to experimental processes that study the effect of a removal or an addition of a particle to the correlated system. As mentioned above, the (e, 2e) process is related to the hole spectral function. In addition, the Green's function allows the evaluation of the expectation value for *any* single-particle operator $\hat{O}$ (this is because $\langle\hat{O}\rangle = \sum_{\alpha\beta}\int_{-\infty}^{E_{\mathrm{F}}} \mathrm{d}\omega S_{\mathrm{h}}(\alpha\beta,\omega)\langle\alpha|O|\beta\rangle$, where $\langle\alpha|O|\beta\rangle$ is the matrix representation of $\hat{O}$ in the basis $|\alpha\rangle$). This in turn highlights the importance of single-particle removal or addition spectroscopies, such as single photoemission [38,39] and (e,2e) processes, which allow insight into the respective part of the Green's function. A further advantage of the Green's function approach is that it offers a systematic way for approximations using the diagram technique [20]. In the diagrammatic expansion for g one introduces the concept of the self-energy Σ [27]. The knowledge of Σ allows the evaluation of g via the Dyson equation

$$g(\alpha\beta;\omega) = g_0(\alpha\beta;\omega) + \sum_{\gamma\delta} g_0(\alpha\gamma;\omega)\Sigma(\gamma\delta;\omega)g(\delta\beta;\omega)\,, \tag{13.34}$$

where g_0 is the Green's function of a (noninteracting) reference system. The self-energy Σ accounts for all excitations due to the interaction of the particle with the surrounding medium and acts as a nonlocal, energy-dependent, and complex single-particle potential.

13.8.2 Particle-Particle and Hole-Hole Spectral Functions

As discussed in detail in [20], the Dyson equation (13.34) can be derived algebraically and the single-particle propagator $g(\alpha t,\alpha' t')$ can be related to the two-particle Green's function $g^{\mathrm{II}}(\beta t_1,\beta' t_1',\gamma t_2,\gamma t_2')$. This is a first cycle in a hierarchy that links the N-particle propagator to the $(N+1)$-particle propagator [36,35]. Of direct relevance to this work is the two-particle propagator $g^{\mathrm{II}}(\beta t_1,\beta' t_1',\gamma t_2,\gamma t_2')$.

Repeating the steps outlined above for the single-particle case, one arrives at the Lehmann representation of the two-particle Green's function in terms of energies and states of the systems with N and $N\pm 2$ particles (the $(N-2)$-particle state of the system is achieved upon a $(\gamma, 2e)$ reaction):

$$g^{\mathrm{II}}(\alpha\beta,\gamma\delta;\Omega) = \sum_n \frac{\langle\Psi_0^{(N)}|a_\beta a_\alpha|\Psi_n^{(N+2)}\rangle\langle\Psi_n^{(N+2)}|a_\gamma^{\dagger}a_\delta^{\dagger}|\Psi_0^{(N)}\rangle}{\Omega - [E_n^{(N+2)} - E_0^{(N)}] + \mathrm{i}\eta} - \sum_m \frac{\langle\Psi_0^{(N)}|a_\gamma^{\dagger}a_\delta^{\dagger}|\Psi_m^{(N-2)}\rangle\langle\Psi_m^{(N-2)}|a_\beta a_\alpha|\Psi_0^{(N)}\rangle}{\Omega - [E_0^{(N)} - E_m^{(N-2)}] - \mathrm{i}\eta}\,. \tag{13.35}$$

Upon analogous considerations made for the one-particle case to arrive at the single-particle spectral functions, one can obtain from g^{II} the hole-hole spectral function as $S_{\mathrm{hh}}(\boldsymbol{k}_1,\boldsymbol{k}_1,\Omega) = \Im g^{\mathrm{II}}(\boldsymbol{k}_1,\boldsymbol{k}_1,\Omega), \Omega \leq 2\epsilon_{\mathrm{F}}/\pi$, which is intimately related to the $(\gamma, 2e)$ reaction.

The two-particle Green's function involves two kinds of diagrams: the first type includes two noninteracting single-particle propagators (see (13.34)) and is supplemented by similar diagrams that include all possible self-energy insertions [3]. The second defines the vertex function Γ. The latter involves all generalization of the lowest-order correction to the two-particle propagator in which two particles interact once. To visualize the role of Γ we write g^{II} in the form

$$\begin{aligned} &g^{\mathrm{II}}(\alpha t_1,\alpha' t_1',\beta t_2,\beta' t_2') \\ &= \mathrm{i}\left[g(\alpha\beta,t_1-t_2)\,g(\alpha'\beta',t_1'-t_2') - g(\alpha\beta',t_1-t_2')\,g(\alpha'\beta,t_1'-t_2)\right] \\ &\quad\times\int \mathrm{d}t_a\mathrm{d}t_b\mathrm{d}t_c\mathrm{d}t_d \sum_{abcd} g(\alpha a,t_1-t_a)\,g(\alpha' b,t_1'-t_b) \\ &\quad\times\langle ab|\Gamma(t_a,t_b;t_c,t_d)|cd\rangle g(c\beta,t_c-t_2)g(d\beta',t_d-t_2')\,. \end{aligned} \tag{13.36}$$

From this equation it is clear that Γ can be considered as the effective interaction between dressed particles. In addition, Γ plays a decisive role in the determination of its single-particle counterpart, the self-energy Σ [3].

In energy-space, the result for the noninteracting (free) product of dressed propagators including the exchange contribution, i.e., the zero-order term of (13.36) with respect to Γ, reads

$$g_{\mathrm{f}}^{\mathrm{II}}(\alpha\beta,\gamma\delta;\Omega) =$$

$$\frac{\mathrm{i}}{2\pi}\int \mathrm{d}\omega\,[g(\alpha,\gamma;\omega)\,g(\beta\,\delta;\Omega-\omega) - g(\alpha,\delta;\omega)\,g(\beta\,\gamma;\Omega-\omega)] =$$

$$\sum_{mm'} \frac{\langle\Psi_0^{(N)}|a_\alpha|\Psi_m^{(N+1)}\rangle\langle\Psi_m^{(N+1)}|a_\gamma^\dagger|\Psi_0^{(N)}\rangle\langle\Psi_0^{(N)}|a_\beta|\Psi_{m'}^{(N+1)}\rangle\langle\Psi_{m'}^{(N+1)}|a_\delta^\dagger|\Psi_0^{(N)}\rangle}{\Omega - \{[E_m^{(N+1)} - E_0^{(N)}] + [E_{m'}^{(N+1)} - E_0^{(N)}]\} + \mathrm{i}\eta} -$$

$$\sum_{nn'} \frac{\langle\Psi_0^{(N)}|a_\gamma^\dagger|\Psi_n^{(N-1)}\rangle\langle\Psi_n^{(N-1)}|a_\alpha|\Psi_0^{(N)}\rangle\langle\Psi_0^{(N)}|a_\delta^\dagger|\Psi_{n'}^{(N-1)}\rangle\langle\Psi_{n'}^{(N-1)}|a_\beta|\Psi_0^{(N)}\rangle}{\Omega - \{[E_0^{(N)} - E_n^{(N-1)}] + [E_0^{(N)} - E_{n'}^{(N-1)}]\} + \mathrm{i}\eta} -$$

$$(\gamma \longleftrightarrow \delta)\,. \tag{13.37}$$

The integration over ω has been carried out by utilizing the Lehmann representation for the single-particle Green's functions. The ladder approximation to the two-particle propagator is

$$g_{\mathrm{L}}^{\mathrm{II}}(\alpha\beta,\gamma\delta;\Omega) = g_{\mathrm{f}}^{\mathrm{II}}(\alpha\beta,\gamma\delta;\Omega) + \frac{1}{4}\sum_{\epsilon\eta\theta\zeta} g_{\mathrm{f}}^{\mathrm{II}}(\alpha\beta,\epsilon\eta;\Omega)\langle\epsilon\eta|V|\theta\zeta\rangle g_{\mathrm{L}}^{\mathrm{II}}(\theta\zeta,\gamma\delta;\Omega)\,, \tag{13.38}$$

where V stands for the naked two-body interaction. This integral relation can now be iterated to yield a set of ladder diagrams. The corresponding ladder sum for the effective interaction Γ, as it appears in (13.36) can be deduced from this result as

$$\langle\alpha_1,\beta_2|\Gamma_{\mathrm{L}}(\Omega)|\alpha_1',\beta_2'\rangle = \langle\alpha_1\beta_2|V|\alpha_1'\beta_2'\rangle + \frac{1}{4}\sum_{\epsilon\eta\theta\zeta}\langle\alpha_1\beta_2|V|\epsilon\eta\rangle g_{\mathrm{f}}^{\mathrm{II}}(\epsilon\,\eta,\theta\,\zeta;\Omega) \times\langle\theta,\zeta|\Gamma_{\mathrm{L}}(\Omega)|\alpha_1',\beta_2'\rangle\,. \tag{13.39}$$

The aforementioned RPA for the particle-hole (polarization) propagator Π means that only the term (13.37) is taken into account. The calculations of higher-order (vertex) corrections entail an evaluation of the sum in (13.38). It is also interesting to contrast (13.38) with the DS3C approach (13.16).

As noticed above, g^{II} is of direct relevance to the $(\gamma, 2\mathrm{e})$ reaction. It should be noted, however, that the ladder approximation (13.38) for the two-particle Green's function can be employed to define the self-energy Σ [20,35], which can then be used to obtain the single-particle Green's function via (13.34). On the other hand, this Green's function enters in the definition of the two-particle Green's function, as is clear, e.g., from (13.37) and (13.38). Thus, in principle, the Dyson (13.34) and (13.38) for the one-body and two-body Green's functions have to be solved in a self-consistent manner. As in the single-particle case where we established the relevance of the spectral representation to the (e,2e) experiments, one can relate g^{II} to the $(\gamma, 2\mathrm{e})$ measurements by means of (13.35): g^{II} shows poles at energies (relative to the ground state) corresponding to adding $[E_n^{(N+2)} - E_0^{(N)}]$ or removing $[E_0^{(N)} - E_n^{(N-2)}]$ two particles from the unperturbed ground state. The residua of these poles are related to the measurable spectroscopic factors for the addition or removal of the two particles, e.g., as done in the $(\gamma, 2\mathrm{e})$ experiment [40]. From the above discussion we conclude thus that $(\gamma, 2\mathrm{e})$ and (e,2e) provide quite different information. On the other hand they are related in as much as the single-particle and the two-particle spectral functions are related to each other.

13.8.3 The Two-Particle Photocurrent

The $(\gamma, 2e)$ experiments from surfaces have been conducted recently [40]. The two-photoelectron current $\mathcal{J}$ is characterized by the wave vectors $\boldsymbol{k}_1$ and $\boldsymbol{k}_2$ of the two photoelectrons. It has the form [41]

$$\mathcal{J} \propto \langle \boldsymbol{k}_1, \boldsymbol{k}_2|g^{\mathrm{IIr}}\Delta S_{\mathrm{hh}}^{\mathrm{II}}(\boldsymbol{k}_1', \boldsymbol{k}_2', E)\Delta^\dagger g^{\mathrm{IIa}}|\boldsymbol{k}_1, \boldsymbol{k}_2\rangle\,, \tag{13.40}$$

where Δ is the dipole operator, $S_{\mathrm{hh}}^{\mathrm{II}}$ is the hole-hole spectral function, and g^{IIa} (g^{IIr}) is the advanced (retarded) two-particle Green's function. As for the single photoemission, the photocurrent can be represented by a two-particle Caroli diagram [41], which explicitly shows no signature of time ordering. This is due to the assumption that the experimental time resolution (typically 200 ns) is much longer than any other timescale in the system and hence a time integration has to be performed to arrive at (13.40). On the other hand, one can tune to initial- or final-state interactions (FSI) by a suitable choice of $\boldsymbol{k}_{1/2}$: if $\boldsymbol{k}_1$ and $\boldsymbol{k}_2$ are very large (compared to the Fermi wave vector), one can expect FSI to be limited to a small region in phase space where the two electrons escape with almost the same velocities. Apart from this regime, FSI become less important, which allows the effect of initial-state correlations to be highlighted. On the other hand, if the two electrons escape with very low (vacuum) velocities, FSI become the determining factor.

Numerical Realization for Metal Surfaces. As is clear from (13.40), the evaluation of g^{II} is the key ingredient for the numerical evaluation of the two-photoelectron current. On the other hand, we have seen in the preceding section that the single-particle Green's function g is needed to obtain g^{II}, and in turn g^{II} goes into the determination of Σ and hence g. Until now this self-consistent loop has been too complicated to be realized numerically within a realistic description of the surface, i.e., for an inhomogeneous electron gas or for a few-electron atomic system.

Incorporating the Single-Particle Band Structure. A possible approach to the evaluation of $\mathcal{J}$ is the following: assuming the two photoelectrons to be independent, then, according to (13.38), the two-particle Green's

function g^{II} reduces to $g^{\mathrm{II}} = g_{\mathrm{f}}^{\mathrm{II}}$. This means, as in the RPA case for Π, g^{II} simplifies to an antisymmetrized product of sp Green's function $g_j(\boldsymbol{k}_i, E_i)$, $i = 1, 2$ that can be used to generate the single-photoelectron states, e.g., by means of the layer Korringa–Kohn–Rostoker (LKKR) method [2]. This method utilizes a density-functional approach [2] combined with a semi-empirical function for the complex part of the self–energy. For the evaluation of $\mathcal{J}$ from metal surfaces one can utilize the interaction potential U_{TF}, with $N(\mu)$ being calculated by the (ab initio) LKKR method. Furthermore, we can write

$$U_{\mathrm{TF}} = \frac{Z_1}{r_1} + \frac{Z_2}{r_2} \quad \text{with} \quad Z_j = a_j^{-1} \exp\left(-\frac{2a_j}{\lambda} r_j\right), \quad j = 1, 2, \qquad (13.41)$$

where $a_j = r_{12}/(2r_j)$. Equation (13.41) indicates that the effect of the electron–electron interaction potential can be viewed as a modification Z_j/r_j to the single-particle potentials. The interelectronic correlation is subsumed into a dynamic nonlocal screening of the interaction w_j of the electron with the lattice. The behavior of this screening is dictated by the functions Z_j, and has the following features: when the two electrons are on top of each other ($r_{12} \to 0$) the potential w_j turns repulsive so as to simulate the strong, short-range electron–electron repulsion. If the two electrons are far away from each other ($r_i \gg r_j$, $i \neq j \in [1, 2]$), the screening strengths Z_1 and Z_2 become negligible and we end up with two independent particles. For the numerical evaluation of the two-photoelectron current Z_j have been approximated by $\bar{Z}_j$, where $\bar{Z}_j = \bar{a}_j^{-1} \exp(-2\bar{a}_j r_j/\lambda)$ and $\bar{a}_j = k_{12}/(2k_j)$. Here, $\boldsymbol{k}_{12} = \boldsymbol{k}_1 - \boldsymbol{k}_2$ is the interelectronic relative wave number. With this screening being included, the modification $\bar{Z}_j/r_j$ to the original single-particle potential w_j can be taken into account and the single-particle Green's function $\bar{g}_j$ is generated. However, in contrast to g, each $\bar{g}_j$ is dependent on the wave vectors of *both* electrons as well as on the mutual, relative wave vector of the escaping electrons. The two-particle Green's function is approximated by $\bar{g}^{\mathrm{II}}$ which is the antisymmetrized, direct product of the modified single-particle Green's functions $\bar{g}_j$ (the first term in the ladder approximation, (13.38)). This model yielded useful results for the (e,2e) cross sections [42–44].

Angular Pair Correlation Functions for Cu(001). Here, the $(\gamma, 2e)$ calculation from Cu(001) are described. The ground-state potentials of the Cu(001) surface are calculated self-consistently with the scalar-relativistic LMTO method. Lifetime broadening of the spectra is simulated by employing a complex optical potential and the photoelectrons' current due to emission from the first 20 outermost layers is calculated. Convergence of the results with respect the maximum angular momentum, number of reciprocal lattice vectors, and accuracy of the energy integration is achieved.

Figure 13.2 shows the angular distributions of the current for single photoemission (labeled SPE) and the double photoemission (indicated by DPE) for an incoming s-polarized photon. The intensity variation is shown as a

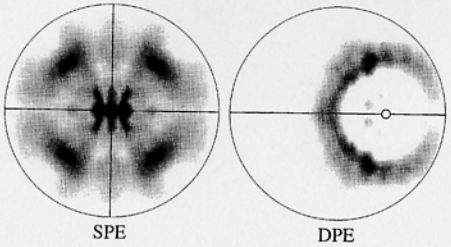

Fig. 13.2. The angular distribution of the photoemission intensity from Cu(001) in single-electron (labeled SPE) and double-electron photoemission (labeled DPE). The kinetic energy of the photoelectrons is 9 eV, the photon energy of the s-polarized light is 15.5 eV in the SPE case whereas in DPE the photon energy is increased to 31 eV as to compensate for the additional energy needed to emit two electrons instead of one. For the DPE case, the small circle indicates the emission direction of one of the electrons (polar angle with respect to the surface normal is $\vartheta = 40°$). Low (high) intensities correspond to *light (dark) gray* scale in the stereographic projection. *Horizontal* and *vertical lines* emphasize the symmetries of the angular distributions

function of the angular position of one photoelectron with 9 eV kinetic energy. The photon energy is 15.5 eV in the single photoemission case and 31 eV for double photoemission. We note that in the latter case both photoelectrons escape with the same kinetic energy of 9 eV. For SPE, the point group of the surface 4 mm is reduced to 2 mm in the angular distribution (as indicated by the horizontal and vertical lines in Fig. 13.2) because the electric-field vector of the incident photon (which lies in a mirror plane of the surface) is not invariant under the operations C_4 and C_4^{-1}. On the other hand in DPE, the group 2 mm is reduced further to m (horizontal line in Fig. 13.2), due to the presence of the second photoelectron. From Fig. 13.2 it is clear that the repulsion between the two escaping photoelectrons leads to a vanishing photoelectron current when the two electrons are close to each other. This is the origin of the *correlation hole* surrounding the fixed detector position. On the other hand, if the two electrons are far from each other, the electron–electron interaction diminishes in strength. Consequently, the two-electron current drops dramatically, for this current must vanish in the absence of correlation. The interplay between these two effects leads to a localization of the angular-intensity distribution of one of the photoelectrons around the position of the second one, as observed in Fig. 13.2. It should be stressed that the two detected photoelectrons are not only coupled to each other but also to the crystal potential. Therefore, the *correlation hole* is not isotropic in space and depends sensitively on the photoelectrons' energies.

13.9 Conclusion

This chapter gives a general overview on the foundations of many-body techniques for the treatment of single and multiple excitations in few and many-body systems. The author's goal has been to emphasis common features and differences when the system size and/or the number of interactions increase. While the wave function approach is well suited for the treatment of few interacting particles it becomes less valuable for large compounds. In the thermodynamic limit the well-established Green's function technique is a powerful tool for the description of correlated excitations in many-body systems.

References

1. D. Pines: Phys. Rev. **92**, 626 (1953); E. Abrahams: Phys. Rev. **95**, 839 (1954); D. Pines, P. Nozieres: *The Theory of Quantum Liquids* (Addison-Wesley, Reading 1966)
2. A. Gonis: *Theoretical Materials Science: Tracing the Electronic Origins of Materials Behavior* (Materials research society, Warrendale 2000)
3. A.L. Fetter, J.D. Walecka: *Quantum Theory of Many-particle Systems* (McGraw-Hill, New York 1971)
4. I. Lindgren, J. Morrison: *Atomic Many-Body Theory* (Springer, Berlin, Heidelberg, New York 1982)
5. L. Rosenberg: Phys. Rev. D **8**, 1833 (1973)
6. M. Brauner, J.S. Briggs, H. Klar: J. Phys. B **22**, 2265 (1989)
7. J.S. Briggs: Phys. Rev. A **41**, 539 (1990)
8. H. Klar: Z. Phys. D **16**, 231 (1990); J. Berakdar: (thesis) University of Freiburg i.Br. (1990) (unpublished)
9. E.O. Alt, A.M. Mukhamedzhanov: Phys. Rev. A **47**, 2004 (1993); E.O. Alt, M. Lieber: ibid. **54**, 3078 (1996)
10. J. Berakdar, J.S. Briggs: Phys. Rev. Lett. **72**, 3799 (1994); J. Phys. B **27**, 4271 (1994)
11. J. Berakdar: Phys. Rev. A **53**, 2314 (1996)
12. S.D. Kunikeev, V.S. Senashenko: Zh.E'ksp. Teo. Fiz. **109**, 1561 (1996); [Sov. Phys. JETP **82**, 839 (1996)]; Nucl. Instrum. Methods B **154**, 252 (1999)
13. D.S. Crothers: J. Phys. B **24**, L39 (1991)
14. G. Gasaneo, F.D. Colavecchia, C.R. Garibotti, J.E. Miraglia, P. Macri: Phys. Rev. A **55**, 2809 (1997); G. Gasaneo, F.D. Colavecchia, C.R. Garibotti: Nucl. Instrum. Methods B **154**, 32 (1999)
15. J. Berakdar: Phys. Lett. A **220**, 237 (1996); ibid. **277**, 35 (2000); Phys. Rev. A **55**, 1994 (1997)
16. R.K. Peterkop: *Theory of Ionisation of Atoms by the Electron Impact*, (Colorado Associated University Press, Boulder 1977)
17. J. Berakdar: Phys. Rev. Lett. **78**, 2712 (1997)
18. J. Berakdar: to be published
19. G.D. Mahan: *Many-Particle Physics*, second edn (Plenum Press, London 1993)
20. A.A. Abrikosov, L.P. Korkov, I.E. Dzyaloshinski: *Methods of Quantum Field Theory in Statistical Physics* (Dover, New York 1975)

21. J. Berakdar: Aust. J. Phys. **49**, 1095 (1996)
22. M. Abramowitz, I. Stegun: *Pocketbook of Mathematical Functions* (Verlag Harri Deutsch, Frankfurt 1984)
23. J. Berakdar: Phys. Rev. Lett. **85**, 4036 (2000)
24. C.N. Yang, T.D. Lee: Phys. Rev. **97**, 404 (1952); ibid. **87**, 410 (1952)
25. S. Grossmann, W. Rosenhauer: Z. Phys. **207**, 138 (1967); ibid. **218**, 437 (1969)
26. M.N. Barber: *Finite-size Scaling* (Phase Transitions and Critical Phenomena) eds. C. Domb, J.L. Lebowity (Academic Press, New York 1983) pp. 145–266
27. L. Hedin: J. Phys. C **11**, R489 (1999)
28. J. Berakdar, O. Kidun, A. Ernst: in *Correlations, Polarization, and Ionization in Atomic Systems*, eds. D.H. Madison, M. Schulz (AIP, Melville, New York 2002) pp. 64–69
29. O. Kidun, J. Berakdar: Phys. Rev. Lett. **87**, 263401 (2001)
30. S. Keller: Eur. Phys. J. D **13**, 51 (2001)
31. S. Matt, B. Dünser, M. Lezius, K. Becker, A. Stamatovic, P. Scheier, T.D. Märk: J. Chem. Phys. **105**, 1880 (1996)
32. V. Foltin, M. Foltin, S. Matt, P. Scheier, K. Becker, H. Deutsch, T.D. Märk: Chem. Phys. Lett. **289**, 181 (1998)
33. S. Keller, E. Engel: Chem. Phys. Lett. **299**, 165 (1999)
34. K.A. Brueckner: Phys. Rev. **97**, 1353 (1955); H.A. Bethe: Ann. Rev. Nucl. Sci. **21**, 93 (1971); J.P. Jeukenne, A. Legeunne, C. Mahaux: Phys. Rep. **25**, 83 (1976)
35. A.B. Migdal: *Theory of Finite Fermi Systems* (Interscience Pub., New York 1967)
36. P.C. Martin, J. Schwinger: Phys. Rev. **115**, 1342 (1959)
37. H. Lehmann: Nuovo Cimento A **11**, 342 (1954)
38. S.D. Kevan (Ed.): *Angle-Resolved Photoemission: Theory and Current Application*, (Studies in Surface Science and Catalysis) (Elsevier, Amsterdam 1992)
39. S. Hüfner: *Photoelectron Spectroscopy* (Springer Series in Solid-State Science, Vol. 82) (Spinger, Berlin, Heidelberg, New York 1995)
40. R. Herrmann, S. Samarin, H. Schwabe, J. Kirschner: Phys. Rev. Lett. **81**, 2148 (1998); J. Phys. (Paris) IV **9**, 127 (1999)
41. N. Fominykh, J. Henk, J. Berakdar, P. Bruno, H. Gollisch, R. Feder: Solid State Commun. **113**, 665 (2000)
42. J. Berakdar, H. Gollisch, R. Feder: Solid State Commun. **112**, 587 (1999)
43. N. Fominykh, J. Henk, J. Berakdar, P. Bruno, H. Gollisch, R. Feder: in *Many-particle Spectroscopy of Atoms, Molecules, Clusters and Surfaces*. Eds. J. Berakdar, J. Kirschner, (Kluwer Acad/Plenum Pub., New York 2001)
44. N. Fominykh, J. Berakdar, J. Henk, P. Bruno: Phys. Rev. Lett. **89**, 086402 (2002)